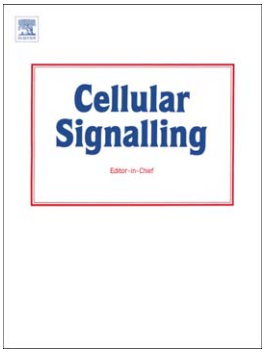

Bortezomib attenuates palmitic acid-induced ER stress, inflammation and insulin resistance in myotubes via AMPK dependent mechanism

Hyun Jeong Kwak, Hye-Eun Choi, Jinsun Jang, Soo Kyung Park, Young-An Bae, Hyae Gyeong Cheon

PII: S0898-6568(16)30067-5
DOI: doi: 10.1016/j.cellsig.2016.03.015
Reference: CLS 8661

To appear in: *Cellular Signalling*

Received date: 31 December 2015
Revised date: 24 March 2016
Accepted date: 28 March 2016

Please cite this article as: Hyun Jeong Kwak, Hye-Eun Choi, Jinsun Jang, Soo Kyung Park, Young-An Bae, Hyae Gyeong Cheon, Bortezomib attenuates palmitic acid-induced ER stress, inflammation and insulin resistance in myotubes via AMPK dependent mechanism, *Cellular Signalling* (2016), doi: 10.1016/j.cellsig.2016.03.015

Bortezomib attenuates palmitic acid-induced ER stress, inflammation and insulin resistance in myotubes via AMPK dependent mechanism

Hyun Jeong Kwak[a], Hye-Eun Choi[a], Jinsun Jang[a], Soo Kyung Park[a], Young-An Bae[b], Hyae Gyeong Cheon[a,c*]

AFFILIATIONS: [a]Department of Pharmacology, Gachon University School of Medicine, Incheon, 406-799, Republic of Korea, [b]Department of Microbiology, Gachon University, Incheon, 406-799, Republic of Korea, [c]Gachon Medical Research Institute, Gil Medical Center, Incheon, 405-760, Republic of Korea

[*]**Correspondence and reprint requests to**:

Hyae Gyeong Cheon, Ph.D.

Professor, Department of Pharmacology

Gachon University School of Medicine

Yeonsu-3 Dong, Yeonsu-Gu, Incheon 406-799

Republic of Korea

Tel: 82-32-820-4761, FAX: 82-32-820-4744

Email: hgcheon@gachon.ac.kr

ABSTRACT

Bortezomib is an anti-cancer agent that induces ER stress by inhibiting proteasomal degradation. However, the effects of bortezomib appear to be dependent on its concentration and cellular context. Since ER stress is closely related to type 2 diabetes, the authors examined the effects of bortezomib on palmitic acid (PA)-induced ER stress in C2C12 murine myotubes. At low concentrations (<20 nM), bortezomib protected myotubes from PA (750 μM)-induced ER stress and inflammation. Either tunicamycin or thapsigargin-induced ER stress was also reduced by bortezomib. In addition, reduced glucose uptake and Akt phosphorylation induced by PA were prevented by co-treating bortezomib (10 nM) both in the presence or absence of insulin. These protective effects of bortezomib were found to be associated with reduced JNK phosphorylation. Furthermore, bortezomib induced AMPK phosphorylation, and the protective effects of bortezomib were diminished by AMPK knockdown, suggesting that AMPK activation underlies the effects of bortezomib. The *in vivo* administration of bortezomib at nontoxic levels (at 50 or 200 μg/kg, *i.p.*) twice weekly for 5 weeks to ob/ob mice improved insulin resistance, increased AMPK phosphorylation, reduced ER stress marker levels, and JNK inhibition in skeletal muscle. The study shows bortezomib reduces ER stress, inflammation, and insulin resistance *in vitro* and *in vivo*, and suggests bortezomib has novel applications for the treatment of metabolic disorders.

Key words; bortezomib, ER stress, AMPK, myotube, insulin resistance

1. Introduction

Bortezomib is an anti-cancer agent that is widely used to treat relapsed/refractory mantle lymphoma and multiple myeloma [1, 2]. It acts as a reversible proteasomal inhibitor specifically targeting 26S proteasome complex [3], and its efficacy relies on the induction of apoptotic cell death by inhibiting IκBα degradation, causing NF-κB inactivation and induction of the JNK pathway [4]. Of the many cell types, myeloma cells appear to be especially sensitive to bortezomib, presumably because these cells rely heavily on the secretory pathway of endoplasmic reticulum (ER), which is sensitive to proteasomal inhibition [5]. Besides its anti-cancer effects, bortezomib has been proposed for the treatment of non-neoplastic diseases, such as, hypertension, arthritis, colitis, asthma, osteoporosis, and ischemia-reperfusion injury [6]. Furthermore, bortezomib has been reported to induce ER stress, to activate unfolded protein response (UPR), and trigger apoptosis and autophagy in several cancer cells [7, 8].

ER serves as a major signal transduction organelle that integrates cellular responses to stress [9]. Under ER stress, cellular defensive mechanisms called UPR are induced to reduce protein synthesis, degrade misfolded proteins, and to restore ER folding capacities. The three main mediators involved in UPR are double-stranded RNA-activated protein kinase (PKR)-like ER kinase (PERK), activating transcription factor 6 (ATF6), and inositol-requiring enzyme-1 (IRE-1α), and all three of these proteins are negatively regulated by chaperone GRP78/BIP in the unstressed normal state [10]. Notably, chronic ER stress may result in impaired Ca^{2+} and redox homeostasis and inflammation, leading to insulin resistance and type 2 diabetes mellitus [11]. Accordingly, type 2 diabetic patients and various animal models of type 2 diabetes have elevated levels of key ER stress markers in pancreas, liver, adipose tissue, and skeletal muscle [10, 12].

Several reports suggest that proteasome inhibition can be protective or apoptotic depending on cell type and inhibitor dosage, and usually switching from a protective to an apoptotic effect exhibits dose dependency [13]. In addition, rapidly proliferating tumor cells are liable to proteasome inhibition-mediated apoptosis, whereas proteasomal inhibitors have been observed to protect various differentiated and quiescent cells from apoptosis [14, 15]. Examples include the protection of endothelial cells from TNFα-induced inflammation by the proteasomal inhibitors MG132 and MG262 [1], and the inhibition of titanium particle-induced inflammation in RAW264.7 cells by bortezomib [16]. However, the underlying mechanisms responsible for the protective effects of proteasomal inhibitors are largely unknown, though it is known that some act by inducing mechanisms other than proteasome inhibition.

Based on reports that bortezomib exerts anti-inflammatory effects in several cell types and also induces ER stress, we investigated its effects on palmitic acid (PA)-induced ER stress and inflammation. We also extended the study to an examination of the effects of bortezomib on tunicamycin and thapsigargin-stimulated ER stress. To this end, we utilized C2C12 murine myotubes which are largely responsible for glucose consumption, and ob/ob mice to assess the *in vivo* effects of bortezomib.

2. Materials and Methods

2.1. Chemicals

Dulbecco's modified Eagle's medium (DMEM), fetal bovine serum (FBS), Dulbecco's phosphate buffered saline (D-PBS), horse serum, penicillin, and streptomycin were obtained from GIBCO (Grand Island, NY). Bortezomib was from LC laboratories (Woburn, MA). Thapsigargin, tunicamycin and palmitic acid were from Sigma Chemical (St. Louis, MO). Antibodies were obtained as follows: Bip/GRP78, ATF6, ATF3, TRB3, CHOP, Akt, pAkt (Ser473), pIRS-1 (Tyr632), ERK, pERK, Glut4 and LKB1 from Santa Cruz Biotechnology (Santa Cruz, CA); AMPK, pAMPK, ACC, pACC, JNK, and pJNK from Cell Signaling Technology (Danvers, MA); pIRS-1 (Ser307) from Bioworld (Minneapolis, MN) and β-actin from Sigma-Aldrich (St. Louis, MO). Oligonucleotide primers were from Bioneer Co. LTD (Daejeon, Korea), and TNF-α and IL-6 ELISA kits from BD Biosciences (San Diego, CA). Protein G Plus-Agarose was from Santa Cruz Biotechnology, and RIPA buffer was from Sigma-Aldrich (St. Louis, MO). All other reagents were from Sigma Chemical (St. Louis, MO) unless indicated otherwise.

2.2. Animals

Male ob/ob mice (5 weeks old) were purchased from the Korean Research Institute of Bioscience and Biotechnology (Ochang, Korea). Animals were acclimated for one week and maintained under constant conditions (20 ± 2°C and humidity 40-60% under a 12 hr light/dark cycle). For experiments, mice were divided into three groups (n=10 per group): Group 1 (the

control group) animals were treated with PBS, Group 2 with bortezomib (50 μg/kg), and Group 3 with bortezomib (200 g/kg) by intraperitoneal (*i.p*) injection twice a week for 5 weeks. Body weights, food intake and blood glucose were measured weekly at the same time every week (between 10:00 and 11:00 AM) for 5 weeks. Food intake was determined by measuring the difference between the preweighed original amount of food and the weight of the food left in each cage (n=5 in each cage). Blood glucose concentrations were determined in tail vein using Allmedicus Gluco Dr. Plus (Seoul) in fed state. All animal procedures were performed in accordance with the Guide for the Care and Use of Laboratory Animals published by the US National Institute of Health (NIH Publication No. 8523, revised 2011) and approved by the Animal Care and Use Committee of Gachon University.

2.3. Cell culture

Mouse C2C12 myoblasts were obtained from the American Type Culture Collection (ATCC, Rockville, MD). Cells were grown in DMEM containing 10% heat-inactivated FBS, penicillin (100 units/ml), and streptomycin sulfate (100 μg/ml) in a humidified 5% CO_2 atmosphere at 37°C. When cells reached confluence, the medium was replaced with differentiation medium containing DMEM and 2% horse serum, which was changed every other day. After four days of incubation, differentiated C2C12 myotubes were pre-treated with indicated concentrations of bortezomib for 1 hr, and then PA (750 μM) was exposed for additional 12 hr (for qPCR) and 24 hr (for western blotting, ELISA and glucose uptake) in the presence or absence of bortezomib. For PA treatment, PA was conjugated with fatty acid-free BSA as described by Chavez et al. [17]. Briefly, PA was completely dissolved in 100% ethanol and then diluted in DMEM containing 2% fatty acid-free BSA. The control treatment was prepared by adding the same amount of ethanol

to BSA-DMEM solution. For tunicamycin or thapsigargin treatment, tunicamycin (1 μg/ml in DMSO, final 0.1% DMSO) or thapsigargin (2 μM in DMSO) was administered to cells for 4 hr in the presence or absence of 10 nM bortezomib. All solutions were filtered, aliquoted, and stored at -20^{o}C prior to use.

2.4. Cell viability assay

Cell viability was determined using MTT assay. Differentiated C2C12 myotubes in 12-well plates were incubated with various concentrations of bortezomib for 1 hr and then exposed to PA (750 μM) for 24 hr. MTT solution (100 μl/well, 5 mg/ml in PBS) was added and cells were incubated for 3 hr. The medium was then replaced with 300 μl/well of DMSO, plates were shaken for 20 min, and optical densities (OD) were measured at 570 nm using a microplate reader (Perkin Elmer VictorX4, Waltham, MA).

2.5. Western blot analysis

Cells or excised tissues were harvested in PRO-PREP™ protein extraction solution (Intron Biotechnology, Korea) and incubated for 30 min at 4°C. Cell debris was removed by microcentrifugation, and supernatants containing proteins were collected. Protein concentrations were determined using Bio-Rad protein assay reagent, according to the manufacturer's instructions. Then, proteins (30 μg) were separated by 10% SDS-polyacrylamide gel electrophoresis (SDS-PAGE), and transferred to PVDF membranes. Blots were incubated with blocking solution (4% BSA) for 1 hr and then incubated overnight with primary antibodies against GRP78, ATF6, ATF3, TRB3, Glut4, p-IRS-1 (Ser307), pIRS-1 (Tyr632), ERK, pERK(Thr202/Tyr204), JNK, pJNK (Thr183/Tyr185), Akt, and p-Akt (Ser473).

After washing with Tween 20/Tris-buffered saline (T-TBS), blots were incubated with horseradish peroxidase-conjugated secondary antibody (1:1000) for 1 hr at room temperature. Membranes were then washed three times with T-TBS and protein bands were detected using an enhanced chemiluminescence kit (Amersham Life Science, Buckinghamshire, UK).

2.6. RNA Preparation and Real-time PCR

Total RNAs from C2C12 cells or excised tissues were isolated using Easy Blue® kits (Intron Biotechnology, Korea). One μg of RNA per sample was reverse-transcribed using ReverTra Ace qPCR RT master mix (Toyobo, Japan). Quantitative real-time PCR (qPCR) was performed by incorporating SYBR green (Toyobo, Japan). The mouse primers used were as follows; GRP78: 5′- CTGGACTGAATGTCATGAGGATCA-3′ (F) and 5′- CTC TTA TCC AGG CCA TAT GCA ATA G-3′ (R), ATF3: 5′-AAC TGG CTT CCT GTG CAC TT-3′ (F) and 5′-TGA GGC CAG CTA GGT CAT CT-3′ (R), CHOP: 5′- CCA CCA CAC CTG AAA GCA GAA-3′ (F) and 5′-GGT GCC CCC AAT TTC ATC T-3′ (R), TRB3: 5′-TCT CCT CCG CAA GGA ACC T-3′ (F) and 5′-TCT CAA CCA GGG ATG CAA GAG-3′ (R), IL-6: 5′-TCT AAT TCA CTT CAA CCA AGA GG-3′ (F) and 5′-TGG TCC TTA GCC ACT CCT TC-3′ (R), TNF-α: 5′-CAT GCA CCA CCA TCA AGG ACT-3′ (F) and 5′- GAG GCA ACC TGA CCA CTC TC-3′ (R), and GAPDH: 5′-CTC AAC TAC ATG GTC TAC ATG TTC CA-3′ (F) and 5′-CCA TTC TCG GCC TTG ACT GT-3′ (R). The mRNA levels were determined using a Roche Light cycler 2.0 (Roche Bio Inc., Switzerland), and results were normalized versus GAPDH.

2.7. AMPK knockdown by siRNA transfection

C2C12 cells were seeded in tissue culture plates ($1x10^5$ cells/well) and differentiated for 24

hr in differentiation medium containing DMEM and 2% horse serum. AMPK siRNA targeting α2 subunit (20 nM, Santa Cruz Biotechnology, Santa Cruz, CA) or negative control siRNA were transfected using Lipofectamine^{TM} RNAiMAX (Invitrogen, Madison, WI) in Opti-MEM medium according to the manufacturer's instructions. Cells were then incubated for 24 hr and media were replaced with differentiation medium. After 48 hr incubation, the differentiated C2C12 cells were treated with the indicated concentrations of bortezomib for 1 hr, followed by 24 hr treatment with PA (750 μM). Extents of AMPK knockdown were determined by Western blotting.

2.8. The 2-NBDG glucose uptake assay

This assay was performed as previously described [18]. Cells ($1x10^4$ cells/well) were seeded in 96-well, clear bottomed, black plates (BD Bioscience, Bedford, MA) and induced to undergo differentiation. Briefly, after 4 days of differentiation, differentiated C2C12 myotubes were pre-treated with 10 nM bortezomib for 1 hr, and then PA (750 μM) was exposed for 24 hr. Cells were changed with serum free/low glucose DMEM containing 20 μM 2-NBDG (2-(N-(7-nitrobenz-2-oxa-1,3-diazol-4-yl)amino)-2-deoxyglucose) (Cayman Chemicals, Arbor, MI) in the absence or presence of 1 μg/ml insulin for 30 min. After washing with PBS, cells were lysed with 70 μl of 0.1 M potassium phosphate (pH 10.0) containing 1% Triton X-100 for 10 min in the dark. DMSO was added to lysates, which were then homogenized by vigorous shaking. Fluorescence was measured using a microplate reader at an excitation wavelength of 480 nm and an emission wavelength of 540 nm (Perkin Elmer VictorX4, Waltham, MA).

2.9. ELISA for TNF-α and IL-6

Levels of TNF-α and IL-6 in culture media were measured using commercially available ELISA kits (BD Biosciences, San Diego, CA).

2.10. Immunoprecipitation of LKB1

Treated cells were lysed in the RIPA buffer, and then, protein (0.5 mg) from cell lysate was immunoprecipitated using rabbit anti-LKB1 antibody (1:100) with prewashed protein G Plus-Agarose overnight. Protein complex were centrifuged at 3,000 rpm for 3 min at 4°C, and the pellets were washed three times with 10 volumes of ice-cold RIPA buffer. The final pellet was added with SDS sample buffer, heated for 5 min at 95°C. After SDS-PAGE and membrane transferring, the membranes were probed with rabbit pAMPK antibody. Separately, the amount of LKB1 in immunoprecipitates was determined by reprobing of the same blot with anti-LKB1 antibody.

2.11. Cytosolic, nuclear and membrane extractions

A subcellular proteome extraction kit (Calbiochem, Inc. San Diego, CA) was used to extract cytosolic and membrane/organelle fractions of differentiated C2C12 cells. Briefly, cells were incubated with various concentrations of bortezomib for 1 hr, exposed to PA (750 μM) for 20 hr, washed twice with PBS, resuspended in 150 μl of ice-cold Extraction I containing 0.75 μl of protease inhibitor mixture, and then incubated for 10 min at 4 °C with gentle agitation. The suspensions obtained were centrifuged at 1000×*g* for 10 min at 4°C. Supernatants were referred to as cytosolic fraction. Pellets were resuspended in 150 μl of ice-cold Extraction II (for membrane fractions) containing 0.75 μl of protease inhibitor mixture, and incubated for 30 min at 4°C. Mixtures were then centrifuged at 6000×*g* at 4 °C, and the supernatants obtained

were referred to as membrane fraction. Remaining pellets were re-suspended in ice-cold Extraction buffer IIII with 0.75 µl of protease inhibitor mixture and incubate for 10 min at 4^{o}C under gentle agitation. Mixtures were then centrifuged at 8800×*g* at 4 °C and supernatants were transferred to the tube as a nuclear fraction.

2.12. Immunofluorescence

Treated cells were washed twice with PBS, fixed for 20 min in 4% paraformaldehyde, washed three times in PBS. Cells were then blocked in 4% normal goat serum containing 0.3% Triton X-100 in PBS for 60 min, which was removed by aspiration before incubating them with a rabbit monoclonal anti-Glut-4 antibody (diluted at 2 µg/ml in BSA buffer) for overnight at 4^{o}C. The cells were then washed three times with PBS, and TRITC-conjugated goat anti-rabbit IgG antibody (Sigma Chemical, St. Louis, MO) at 5 µg/ml in PBS for 60 min at room temperature. After rinses with PBS twice, cells were counterstained with 4', 6-diamidino-2-phenylindole (DAPI) in mounting medium (Vector Laboratories, Burlingame, CA). Cover slips were mounted on microscope slides and images were obtained using an Olympus LG-PS2 microscope (Tokyo).

2.13. Oral glucose tolerance testing (OGTT) and insulin tolerance testing (ITT)

OGTT and ITT were conducted after 5 weeks of bortezomib treatment. For OGTT, mice were fasted for 16 hr (from 5:00 PM to 9:00 AM, only water was supplied for all mice) prior to testing and then given an oral injection of D-glucose (2 g/kg). Blood glucose was measured by tail bleeds at the indicated time points for up to 120 min after glucose administration. After 3 days, ITT was done similarly, except the mice were fasted for only 4 hr (from 9:00 AM to 1:00

PM, only water was supplied for all mice) and 0.75 IU/kg insulin (Sigma Chemical, St. Louis, MO) was administered by *i.p.* injection. Bloods samples were taken from tail veins at the indicated times for up to 120 min after insulin administration, and blood glucose levels were measure using an Allmedicus Gluco Dr. Plus (Seoul). The area under the curve (AUC) for glucose was calculated for the OGTT or ITT using software OriginPro 6.1 (Origin, Northampton, MA)

2.14. Tissue preparation and analysis

After ITT, mice were sacrificed, and tissues, including subcutaneous, visceral, and reproductive fats were removed, rinsed with phosphate buffered saline (PBS), and weighed. For RNA and protein extraction, tissues were frozen rapidly, and stored in liquid nitrogen until required.

2.15. Statistical analysis

The significances of differences versus respective controls were determined using the Student′s *t*-test for paired experiments or two-way ANOVA. Results are presented as the means ± SD of three separate experiments, and p values of < 0.05 were considered statistically significant.

3. Results

3.1. Effects of bortezomib on ER stress and inflammation in C2C12 myotubes

To evaluate the effects of bortezomib on ER stress and inflammation, we treated C2C12 myotubes with various concentrations of bortezomib (1-100 nM), and examined its effects on the expression of ER stress markers and proinflammatory cytokines. As shown in Figs. 1A and B, bortezomib had little effect on the expressions of ER stress markers at concentrations up to 20 nM, but significantly increased ATF6, ATF3, GRP78, CHOP, and TRB3 mRNA and protein levels at higher concentrations. Likewise, proinflammatory cytokine productions by bortezomib were concentration dependent and showed marked induction from 50 nM (Fig. 1C). Bortezomib did not exhibit any cytotoxicity at the concentrations used in the present study (1-100 nM) (Fig. 1D).

3.2. Low dose bortezomib protected C2C12 myotubes from PA-induced ER stress and inflammation

As was expected, C2C12 myotubes exposed to PA (750 μM) displayed increased ER stress marker levels (ATF6, ATF3, GRP78, CHOP, TRB3) as compared with cells exposed to BSA alone (Figs. 2A and B). To examine the effects of bortezomib on PA-induced ER stress, we added bortezomib at concentrations of < 20 nM, at which it did not induce ER stress. In contrast to PA treatment alone, co-incubation of cells with PA and bortezomib (0.1-20 nM) concentration-dependently reduced the expressions of ER stress markers induced by PA (Figs.

2A and B), suggesting that bortezomib prevented PA-induced ER stress. In addition, PA induced inflammatory responses in myotubes, as determined by TNF-α and IL-6 production, and this increase was partially prevented by co-treatment with bortezomib (Fig. 2C) (TNF-α: maximum reduction of 38.0 ± 4.0% by ELISA and maximum mRNA reduction of 29.2 ± 0.97%; IL-6: maximum reduction of 69.0 ± 10.0% by ELISA and maximum mRNA reduction of 85.4 ± 0.70%). Furthermore, these protective effects of bortezomib from PA-induced ER stress and inflammation was not attributed to the increased cell viability since bortezomib′s concentrations used in the present study had little effect on cell viability (results not shown).

To confirm the protective effect of bortezomib on ER stress, we induced ER stress with either tunicamycin or thapsigargin, two well-known inducers of ER stress. Both tunicamycin (1 μg/ml) and thapsigargin (2 μM) increased the mRNA levels of ER stress markers, but these increases were lessened by bortezomib (10 nM) co-treatment (Figs. 3A and B), indicating that low dose bortezomib protects against ER stress regardless of the stress-inducing agent used.

3.3. Low dose bortezomib protected C2C12 myotubes from PA-induced insulin resistance

Given the associations between ER stress, inflammation and insulin resistance, we next examined the effects of bortezomib on Akt phosphorylation in C2C12 cells. PA treatment reduced both basal and insulin-stimulated Akt phosphorylation, which was reversed by co-treating bortezomib (10 nM) (Fig. 4A). Correspondingly, glucose uptake was increased by 49.1 ± 1.36% in the presence of insulin (1 μg/ml), and this increased glucose uptakes were reduced by PA (35.6 ± 5.85% reduction). Bortezomib (10 nM) co-treatment completely prevented PA-

mediated reduction of glucose uptakes (Fig. 4B), which was further confirmed by increased Glut4 translocation to plasma membrane in the presence of bortezomib, as indicated by western blot (Fig. 4C) and by TRITC-conjugated Glut4 (indicated by white arrows) (Fig. 4D). On the other hand, bortezomib (10 nM) had little effect on insulin-stimulated glucose uptake when administered alone, and showed similar effects regardless of insulin presence. Cytochalasin B (CB, 10 μM), an inhibitor of glucose transport almost completely inhibited glucose uptake, validating the assay condition.

To access the mechanisms responsible for the protective effect of bortezomib against PA-induced ER stress, we examined the JNK pathway. PA treatment induced JNK phosphorylation, whereas co-treatment of myotubes with PA plus bortezomib decreased JNK phosphorylation, in parallel with reduced IRS-1 serine (307) phosphorylation, suggesting that the inhibition of JNK phosphorylation is involved in the suppressive action of bortezomib. In parallel, PA-reduced tyrosine phosphorylation of IRS-1 was recovered by bortezomib both in the presence or absence of insulin. ERK phosphorylation was unaffected by either PA alone or bortezomib co-treatment (Fig. 4E).

3.4. Involvement of AMPK activation in the effects of bortezomib in C2C12 myotubes

AMPK activation is a key protective mechanism against PA-induced insulin resistance in myotubes. Here, to elucidate the role played by AMPK in the protective effects of bortezomib, we measured AMPK phosphorylation after incubation with PA in the presence or absence of bortezomib. Incubation with PA alone decreased AMPK and ACC phosphorylation, but this was not observed after co-incubation with PA and bortezomib (Fig. 5A), which suggested that

AMPK activation may contribute to the protective effect of bortezomib against PA-induced ER stress. Since AMPK phosphorylation is known to be induced by LKB1, we further examined the interaction between AMPK and LKB1 by coimmunoprecipitation. Indeed, the association between LKB1 and AMPK, and thus AMPK phosphorylation was enhanced in the presence of bortezomib (Fig. 5B). AICAR (AC) was used as a positive control for LKB1 and AMPK interaction.

Confirmation of AMPK involvement was supported by an AMPK knockdown experiment. Transfection of C2C12 myotubes with AMPK siRNA reduced the expression of AMPK by 68.7 ± 7.4% (Fig. 5C), and increases in the phosphorylations of AMPK by bortezomib was abolished by AMPK knockdown (Fig. 5D). Consistently, AMPK knockdown prevented bortezomib inhibition of the PA-induced expressions of ER stress markers (Figs. 5E) and inflammatory response markers (Fig. 5F), and the PA-induced suppression of insulin-stimulated glucose uptake (Fig. 5G). These findings suggest that AMPK activation is a critical participant in the mechanism responsible for the protective effects of bortezomib against PA-induced ER stress, inflammation, and insulin signaling. On the other hand, increased JNK phosphorylation by PA was unaffected by AMPK knockdown (Fig. 5D), suggesting that inhibition of JNK activation by bortezomib is an independent mechanisms from AMPK phosphorylation.

3.5. In vivo effects of bortezomib in ob/ob mice

To examine the *in vivo* effects of bortezomib, we intraperitoneally administered bortezomib (50 or 200 μg/kg) to *ob/ob* mice twice weekly for 5 weeks. As shown in Fig. 6A, bortezomib lowered blood glucose levels as compared with vehicle controls (a comparison of AUCs showed

27.9 ± 9.8% inhibition by bortezomib at 200 μg/kg) and in parallel improved glucose intolerance as determined by OGTT and ITT; based on AUC calculations of OGTT and ITT curves, 18.8 ± 5.7% and 23.1 ± 7.1% inhibitions, respectively, were obtained at a bortezomib concentration of 200 μg/kg. In parallel with the reduction of glucose levels, there was a significant decrease in proinflammatory cytokines both in plasma and skeletal muscles (Fig. 6B and C), which suggested bortezomib improves insulin sensitivity in *ob/ob* mice. On the other hand, plasma adiponectin was unchanged after bortezomib treatment (results not shown). At 200 μg/kg of bortezomib, reduced body weights and fat weights were observed without affecting food intake rate (results not shown), which may be due to either direct effects on adipose tissue or indirect effects via crosstalk between skeletal muscle and adipose tissue.

When we examined the effects of bortezomib on ER stress in skeletal muscle, we found that the levels of ER stress markers were significantly reduced in bortezomib-treated animals as compared with vehicle controls (Fig. 6D). Furthermore, after bortezomib administration, increased phosphorylations of AMPK and Akt, and decreased JNK phosphorylation were observed in skeletal muscle (Fig. 6E). Taken together, these results indicate bortezomib protects against PA-induced ER stress, inflammation, and insulin resistance in murine myotubes by inhibiting JNK and activating AMPK, and suggest that the therapeutic applications of bortezomib could be further extended.

4. Discussion

Bortezomib is a known inducer of ER stress and of tumor cell apoptosis [5, 7, 8]. The present study shows that bortezomib at low concentrations protects murine skeletal muscle cells from PA-induced ER stress, inflammation, and insulin resistance, and improves insulin resistance in ob/ob mice. AMPK activation by bortezomib appears to be a key component of the mechanism underlying the protective action of bortezomib. A proposed model of the mechanism responsible for the effects of bortezomib is presented in Fig. 7.

The ubiquitin-proteasome system plays a central role in many cellular functions, such as, the cell cycle, apoptosis, cell adhesion, inflammatory processes, angiogenesis, and immune response, and proteasomal dysfunction contributes to the development of disease states [19]. For these reasons, proteasome inhibitors have been applied to numerous clinical therapies, especially for the treatment of various malignant diseases. Bortezomib, which is perhaps the best known proteasomal inhibitor, exerts broad anti-tumor activities, and has been approved as a cytostatic drug for the treatment of multiple myeloma based on favorable clinical trial results [2]. On the other hand, recent reports indicate proteasome inhibitors have diverse effects on nonmalignant cells, and that their effects depend on cell type and dosage. For example, proteasome inhibition sensitizes hepatocellular carcinoma cells, but not human hepatocytes [15]. In addition, biphasic dosage effects have been reported for proteasome inhibitors in different cells, including astrocytes and endothelial cells, whereby they afford protection at low doses and induce apoptosis at high doses [20, 21].

Bortezomib and other proteasome inhibitors have anti-inflammatory effects attributable to the attenuation of NF-κB activation. NF-κB is sequestered in cytoplasm as a complex by its

inhibitor IκB under resting conditions, and is activated by IκB release by 26S proteasome-mediated IκB degradation upon stimulation. Thus, proteasome inhibition stabilizes IκB, and thus, reduces its release from NF-κB [22]. However, several authors have suggested the varied effects of bortezomib in non-cancerous cells are independent of NF-κB inhibition. For example, the anti-inflammatory effects of bortezomib in endothelial cells are mediated by anti-oxidant effects and not by NF-κB inhibition [23], and the protective effects of bortezomib against lung and skin fibrosis appear to be mediated by increased PPARγ abundance and activity [24]. However, the mechanisms responsible for the protective effects of proteasome inhibition by bortezomib are largely unknown.

Lipotoxicity induced by high concentrations of circulating saturated fatty acids is a key mechanism of insulin resistance development, and of these fatty acids, PA is the most prevalent. PA impairs insulin signaling through numerous mechanisms including ER stress and oxidative stress in a cell type dependent manner [25], and this effect of PA appears to be mediated by its metabolites because non-metabolizable methylpalmitate has been reported not to induce ER stress [26, 27]. In hypothalamic neurons, PA was found to induce ER stress via a JNK dependent pathway [28], whereas in skeletal muscle, ER stress may be caused by differential lipid composition and localization by PA [29]. Although it has been reported that PA-induced insulin resistance is independent of ER stress in skeletal muscle cells, we observed PA induced ER stress and insulin resistance and that both were alleviated by bortezomib at low doses. Reasons for discrepancies between these studies remain unclear.

Close link between inflammation and insulin resistance has been confirmed in many studies. Of note, the levels of proinflammatory cytokines (TNF-α, IL-1, and IL-6) increased in type 2 diabetes, and among those, IL-6 strongly correlates with insulin resistance and type 2

diabetes [30, 31]. Accordingly, our results showed that bortezomib attenuated palmitate-induced inflammation in C2C12 cells by decreasing the production of proinflammatory cytokines. Similar to our findings, oleate reduced palmitate-induced production of proinflammatory cytokines in C2C12 cells, in association with improved insulin resistance [32]. Different from conventional thoughts on IL-6 as a proinflammatory cytokine, recent studies suggested that IL-6, acting as a major myokine, may have beneficial effects in the metabolic context [33, 34], which deserves further research to clarify on the role of IL-6 in metabolic disorders.

In the present study, bortezomib up to 100 nM did not induce cytotoxicity as determined by MTT assay, but a previous study reported that bortezomib inhibited C2C12 cell growth in the concentration range 1-40 nM [35]. Differences in the sensitivities of C2C12 cells to bortezomib may due to differences in differentiation state (myoblast *vs.* myotube). In the present study, bortezomib had little effect on C2C12 myotube viability, and at low concentrations (<20 nM), reduced PA-induced ER stress in C2C12 cells via novel mechanisms, i.e. AMPK activation. AMPK is an AMP-activated protein kinase and acts as a cellular energy sensor. Its activation induces catabolic pathways and the generation of ATP under conditions of hypoxia and nutrient deprivation [36]. AMPK has also been reported to be involved in the prevention of PA-induced JNK phosphorylation and ER stress [28]. In the present study, bortezomib increased AMPK and Akt phosphorylation, but and led to a reduction in JNK activation. Since AMPK knockdown was found to abolish the protective effects of bortezomib, AMPK appears to be a key mediator of its action. Consistent with previous reports [23], bortezomib also reduced PA-induced ROS production (results not shown), which might also have contributed to its amelioration of ER stress and insulin resistance. Like bortezomib, oleate and PPARβ/δ agonists

have been reported to prevent PA-induced ER stress, inflammation, and insulin resistance via AMPK activation [37, 38]. These results with those of the present study suggest that AMPK activation is a critical requirement for protection from the lipotoxic effects of PA.

AMPK activation by bortezomib has been previously reported in different cell types. In cultured pancreatic and colorectal cancer cells, bortezomib (100 nM) induced AMPK phosphorylation, whereas AMPK inhibition or knockdown suppressed bortezomib-induced autophagy and had an anti-apoptotic effect on cancer cells [39]. Bortezomib has also been reported to induce AMPK activation in Sertoli cells and interfere with the normal development of germ cells [40]. Thus, the consequences of AMPK activation by bortezomib appear to depend on cell type, the cellular environment, and bortezomib concentration. However, how bortezomib induces AMPK phosphorylation at the molecular level remains to be elucidated, and the mechanism involved may not be related to proteasome inhibition.

To examine the validity of our *in vitro* observations *in vivo*, we examined the effects of bortezomib in *ob/ob* mice, which are known to exhibit elevated levels of key markers of ER stress. Bortezomib administration (200 μg/kg, twice a week) for five weeks reduced the expressions of ER stress markers and increased AMPK phosphorylation in skeletal muscles. Furthermore, bortezomib increased insulin sensitivity and lowered plasma glucose levels, which suggests bortezomib reduced ER stress and acted to restore insulin sensitivity. These findings indicate bortezomib should be examined for possible use as an anti-diabetics after the dosage range is clearly defined with respect to protection against ER stress and insulin resistance.

5. Conclusion

Contrary to the original hypothesis that bortezomib acts as an ER stress inducer, our study indicates that bortezomib at low concentrations reduces ER stress and insulin resistance. AMPK activation is a possible mechanism underlying the protective effects of bortezomib against PA-induced ER stress, but other pathways might also participate, and this deserves further investigation. The mitigation of ER stress is a topic of considerable therapeutic significance in the context of metabolic disorders. In this regard, we suggest further studies be undertaken to resolve the side effects associated with bortezomib and to establish its clinical relevance with respect to the treatment of metabolic disorders.

6. References

[1] R.I. Fisher, S.H. Berstein, B.S. Kalh, B. Djulbegovic, M.J. Robertson, V.S. Epner, J.P. Krishnan, S. Leonard, F.A. Lonial, O.A. Stadtmauer, H.S. O'Connor, A.L. Boral, A. Goy, Multicenter phase II study of bortezomib in patients with relapsed or refractory mantle cell lymphoma, J. Clin. Oncol. 24 (2006) 4867-4874.

[2] P.G. Richardson, B. Barlogie, J. Berenson, S.S. Inghal, S. Jagannath, D. Irwin, S.V. Rajkumar, G. Srkalovic, M. Alsina, R. Alexanian, D. Siegel, R.Z. Orlowski, D. Kuter, S.A. Limentani, S. Lee, T. Hideshima, D.L. Esseltine, M. Kauffman, J. Adams, D.P. Schenkein, K.C. Anderson, A phase 2 study of bortezomib in relapsed, refractory myeloma. N. Engl. J. Med. 348 (2003) 2609-2617.

[3] P.F. Bross, R. Kane, A.T. Farrell, S. Abraham, K. Benson, M.E. Brower, S. Bradle, J.V. Gobburu, A.M. Goheer, S.L. Lee, J. Leighton, C.Y. Liang, R.T. Lostritto, W.D. McGuinn, D.E. Morse, A. Rahman, L.A. Rosario, S.L. Verbois, G. Williams, Y.C. Wang, R. Pazdur, Approval summary for bortezomib for injection in the treatment of multiple myeloma, Clin. Cancer Res. 10 (2004) 3954-3964.

[4] S. Meiners, A. Ludwig, V. Stangl, K. Stangl, Proteasome inhibitors: poisons and remedies, Med. Res. Rev. 28 (2008) 309-327.

[5] E.A. Obeng, L.M. Carlson, D.M. Gutman, W.J. Jr. Harrington, K.P. Lee, L.H. Boise, Proteasome inhibitors induce a terminal unfolded protein response in multiple myeloma cells, Blood 107 (2006) 4907-4916.

[6] J. Wang, M.A. Maldonado, The ubiquitin-proteasome system and its role in inflammatory and autoimmune diseases, Cell Mol. Immunol. 3 (2006) 255-261.

[7] T. Otoda, T. Takamura, H. Misu, T. Ota, S. Murata, H. Hayashi, H. Takayama, A. Kikuchi, T. Kanamori, K.R. Shima, F. Lan, T. Takeda, S. Kurita, K. Ishikura, Y. Kita, K. Iwayama, K.M. Kato, M. Uno, Y. Takeshita, M. Yamamoto, K. Tokuyama, S. Iseki, K. Tanaka, S. Kaneko, Proteasome dysfunction mediates obesity-induced endoplasmic reticulum stress and insulin resistance in the liver, Diabetes 62 (2013) 811-824.

[8] D. Selimovic, B.B. Porzig, A. El-Khattouti, H.E. Badura, M. Ahmad, F. Ghanjati, S. Santourlidis, Y. Haikel, M. Hassan, Bortezomib/proteasome inhibitor triggers both apoptosis and autophagy-dependent pathways in melanoma cell, Cell Signal. 25 (2013) 308-318.

[9] N. Chaudhari, P. Talwar, A. Parimisetty, C.L. d'Hellencourt, P. Ravanan P, A molecular web: endoplasmic reticulum stress, inflammation, and oxidative stress, Front. Cell Neuroscience 8 (2014) 1-15.

[10] U. Ozcan, Q. Cao, E. Yilmaz, A.H. Lee, N.N. Iwakoshi, E. Ozdelen, G. Tuncman, C. Gorgun, L.H. Glimcher, G.S. Hotamisligil, Endoplasmic reticulum stress links obesity, insulin action and type 2 diabetes, Science 313 (2006) 1137-1140.

[11] G.S. Hotamisligil, Endoplasmic reticulum stress and the inflammatory basis of metabolic disease, Cell 140 (2010) 900-917.

[12] P. Marchetti, M. Bugliani, R. Lupi, L. Marselli, U. Boggi, F. Filipponi, G.C. Weir, D.L. Eizirik, M. Cnop, The endoplasmic reticulum in pancreatic beta cells of type 2 diabetes patients, Diabetologia 50 (2007) 2486-2494.

[13] S. Meiners, A. Ludwig, M. Lorenz, H. Dreger, G. Baumann, V. Stangl, K. Stangl, Nontoxic proteasome inhibition activates a protective antioxidant defense response in endothelial cells, Free Radic. Biol. Med. 40 (2006) 2232-2241.

[14] H.C. Drexler, Activation of the cell death program by inhibition of proteasome function, Proc. Natl. Acad. Sci. USA 94 (1997) 855-860.

[15] T.M. Ganten, R. Koschny, T.L. Haas, J. Sykora, M. Li-Weber, K. Herzer, H. Walczak, Proteasome inhibition sensitizes hepatocellular carcinoma cells, but not human hepatocytes, to TRAIL, Hepatology 42 (2005) 588-597.

[16] X. Mao, X. Pan, X. Peng, T.M. Cheng, X. Zhang, Inhibition of titanium particle-induced inflammation by the proteasome inhibitor bortezomib in murine macrophage-like RAW264.7 cells, Inflammation 35 (2012) 1411-1418.

[17] J.A. Chavez, T.A. Knotts, L.P. Wang, G. Li, R.T. Dobrosky, G.I. Florant, S.A. Summers, A role for ceramide, but not diacylglycerol, in the antagonism of insulin signal transduction by saturated fatty acids, J. Biol. Chem. 278 (2003) 10297-10303.

[18] D.W. Jung, H.H. Ha, X. Zheng, Y.T. Chang, D.R. Williams, Novel use of fluorescent glucose analogues to identify a new class of triazine-based insulin mimetics possessing useful secondary effects. Mol. Biosyst. 7 (2011) 346-358.

[19] A.L. Goldberg, Protein degradation and protection against misfolded or damaged proteins, Nature 426 (2003) 895-899.

[20] M. Stasiolek, V. Gavrilyuk, A. Sharp, P. Horvath, K. Selmaj, D.L. Feinstein, Inhibitory and stimulatory effects of lactacystin on expression of nitric oxide synthase type 2 in brain glial cells. The role of Ikappa N-beta, J. Biol. Chem. 275 (2000) 24847-24856.

[21] V. Stangl, M. Lorenz, S. Meiners, A. Ludwig, C. Bartsch, M. Moobed, A. Vietzke, H.T. Kinkel, G. Baumann, K. Stangl, Long term up-regulation of eNOS and improvement of endothelial function by inhibition of the ubiquitin-proteasome pathway, FASEB J. 18 (2004) 272-279.

[22] M. Karin, Y. Ben-Neriah, Phosphorylation meets ubiquitination: the control of NF-kapaB activity, Annu. Rev. Immunol. 18 (2000) 621-623.

[23] A. Ludwig, M. Fechner, N. Wilck, S. Meiners, N. Grimbo, G. Baumann, V. Stangl, K. Stangl, Potent anti-inflammatory effects of low-dose proteasome inhibition in the vascular system, J. Mol. Med. 87 (2009) 793-802.

[24] G.M. Mutlu, G.R. Budinger, M. Wu, A.P. Lam, A. Zirk, S. Rivera, D. Urich, S.E. Chiarella, L.H.T. Go, A.K. Ghosh, M. Selman, A. Pardo, J. Varga, D.W. Kamp, N.S. Chandel, J.L. Sznajder, M. Jain, Proteasomal inhibition after injury prevents fibrosis by modulating TGF-β(1) signaling, Thorax 67 (2012) 139-146.

[25] E.J. Park, A.Y. Lee, S. Park, J.H. Kim, M.H. Cho, Multiple pathways are involved in palmitic acid-induced toxicity. Food Chem. Toxicol. 67 (2014) 26-34.

[26] D.A. Cunha, P. Hekerman, L. Ladriere, A. Bazarra-Castro, F. Ortis, M.C. Wakeham, F. Moore, J. Rasschaert, A.K. Cardozo, E. Bellomo, L. Overbergh, C. Mathieu, R. Lupi, T. Hai, A. Herchuelz, P. Marchetti, G.A. Rutter, D.L. Eizirik, M. Cnop, Initiation and execution of lipotoxic ER stress in pancreatic β cells, J. Cell Sci. 121 (2008) 2308-2318.

[27] I. Briaud, J.S. Harmon, C.L. Kelpe, V.B. Segu, V. Poitout, Lipotoxicity of pancreatic β cell is associated with glucose-dependent esterification of fatty acids into neutral lipids, Diabetes 50 (2001) 315-321.

[28] C.M. Mayer, D.D. Belsham, Palmitate attenuated insulin signaling and induces endoplasmic reticulum stress and apoptosis in hypothalamic neurons: Rescue of resistance and apoptosis through adenosine 5’ monophosphate-activated protein kinase activation, Endocrinology 151 (2010) 576-585.

[29] G. Peng, L. Li, Y. Liu, J. Pu, S. Zhang, J. Yu, J. Zhao, P. Liu P, Oleate blocks palmitate-

induced abnormal lipid distribution, endoplasmic reticulum expansion and stress, and insulin resistance in skeletal muscle, Endocrinology 152 (2011) 2206-2218.

[30] J.C. Pickup, M.B. Mattock, G.D. Chusney, D. Burt, NIDDM as a disease of the innate immune system: association of acute-phase reactants and interleukin-6 with metabolic syndrome X. Diabetologia 40 (1997) 1286-1292.

[31] A.D. Pradhan, J.E. Manson, N. Rifai, J.E. Buring, P.M. Ridker, C-reactive protein, interleukin 6 and risk of developing type 2 diabetes mellitus. JAMA 286 (2001) 327-334.

[32] T. Coll, E. Eyre, R. Rodriguez-Calvo, X. Palomer, R.M. Sanchez, M. Merlos, J.C. Laguna, M. Vazquez-Carrera, Oleate reverses palmitate-induced insulin resistance and inflammation in skeletal muscle cells. J. Biol. Chem. 283 (2008) 11107-11116.

[33] M. Pal, M.A. Febbraio, M. Whitham, From cytokine to myokine: the emerging role of interleukin-6 in metabolic regulation. Immunol. Cell Biol. 92 (2014) 331-339.

[34] B.K. Pedersen, M.A. Febbraio, Muscles, exercise and obesity: skeletal as a secretory organ. Nat. Rev. Endocrinol. 8 (2012) 457-463.

[35] S.S. Xing, C.C. Shen, M.P. Godard, J.J. Wang, Y.Y. Yue, S.T. Yang, Q. Zhao, S.B. Zhang, T.X. Wang, X.L. Yang, P. Delafontaine, Y. He, Y.H. Song, Bortezomib inhibits C2C12 growth by inducing cell cycle arrest and apoptosis. Biochem. Biophys. Res. Commun. 445 (2014) 375-380.

[36] D.G. Hardie, AMP-activated/SNF1 protein kinase: conserved guardians of cellular energy, Nat. Rev. Mol. Cell Biol. 8 (2007) 774-785.

[37] L. Salvado, T. Coll, A.M. Gomez-Foix, E. Salmeron, E. Barroso, X. Palomer, M. Vazquez-Carrera, Oleate prevents saturated-fatty acid-induced ER stress, inflammation and insulin resistance in skeletal muscle cells through an AMPK-dependent mechanism, Diabetologia

56 (2013) 1372-1382.

[38] L. Salvado, E. Barroso, A.M. Gomez-Foix, X. Palomer, L. Michalik, W. Wahli, M. Vazquez-Carrera, PPARβ/δ prevents endoplasmic stress-associated inflammation and insulin resistance in skeletal muscle cells through AMPK-dependent mechanism, Diabetologia 57 (2014) 2126-2135.

[39] H. Min, M. Xu, Z. Chen, J. Zhou, M. Huang, K. Zheng, X. Zou, Bortezomib induces protective autophagy through AMP-activated protein kinase activation in cultured pancreatic and colorectal cancer cells, Cancer Chemother. Pharmacol. 74 (2014) 167-176.

[40] W. Li, J. Fu, S. Zhang, J. Zhao, N. Xie, G. Cai, The proteasome inhibitor bortezomib induces testicular toxicity by upregulation of oxidative stress, AMP-activated protein kinase (AMPK) activation and deregulation of germ cell development in adult murine testis, Toxicol. Applied. Pharmacol. 285 (2015) 98-109.

Acknowledgements

This research was supported by the intramural research fund of Gachon University (project no. GCU-2015-5106) and by a grant of the Korea Health Technology R&D Project through the Korea Health Industry Development Institute (KHIDI), funded by the Ministry of Health & Welfare, Republic of Korea (grant number: HI14C1135).

Conflicts of interests

The authors declare no conflicts of interest

Contributors

HJK researched data and wrote the manuscript. HEC researched data and reviewed manuscript. JJ and SKP researched data. YAB researched data, contributed to discussion and reviewed manuscript. HGC wrote and edited manuscript. HGC is the guarantor of this work and, as such, had full access to all the data in the study and takes responsibility for the integrity of the data and the accuracy of the data analysis.

Figure legends

Fig. 1. Effects of bortezomib on ER stress and inflammation. Differentiated C2C12 myotubes were exposed to different concentrations of bortezomib (B: 1-100 nM) for 12 hr (for qPCR) and 24 hr (for western blotting and ELISA) and the expression levels of ER stress markers were then determined by western blotting (A) and qPCR (B). Levels of proinflammatory cytokines were determined by ELISA and qPCR (C). Cell viabilities were determined by MTT assay (D). Results are expressed as means ± SD of three experiments in triplicates. **P*<0.05 *vs.* non-treated controls.

Fig. 2. Cytoprotective effects of bortezomib on PA-induced ER stress and inflammation. Differentiated C2C12 myotubes were exposed to low concentrations of bortezomib (0.1-20 nM) for 1 hr and then to PA (750 μM) in the presence of bortezomib for 12 hr (for qPCR) and 24 hr (for western blotting and ELISA). The expression levels of ER stress markers were determined by western blotting (A) and qPCR (B). Levels of proinflammatory cytokines were determined by ELISA and qPCR (C). Results are expressed as the means ± SD of three experiments performed in triplicate. #*P*<0.05 *vs.* non-treated controls, **P*<0.05 *vs.* PA alone.

Fig. 3. Cytoprotective effects of bortezomib on tunicamycin or thapsigargin-induced ER stress. Differentiated C2C12 myotubes were exposed to 10 nM bortezomib for 1 hr, and then to tunicamycin (1 μg/ml; A) or thapsigargin (2 μM; B) for 4 hr in the presence of bortezomib. The expression levels of ER stress markers were determined by qPCR. Results are expressed as the

means ± SD of three experiments performed in triplicate. #P<0.05 *vs.* non-treated controls (0.1% DMSO), *P<0.05 *vs.* tunicamycin alone or thapsigargin alone.

Fig. 4. Mechanisms believed to underlie the effects of bortezomib. Differentiated C2C12 myotubes were exposed to bortezomib (10 nM) for 1 hr, and then to PA (750 μM) for 24 hr, followed by incubation with or without insulin (1 μg/ml) for 30 min. Akt phosphorylation (A) and glucose uptake (B) were determined by western blotting and by 2-NBDG, respectively. Glut4 translocation to plasma membrane was detected by western blot (C), and by immunofluorescence (D). The merged images obtained from overlaying the TRITC-conjugated Glut4 (red) with the nucleus staining by DAPI (blue) were presented, and white arrows indicate Glut4 translocation. Western blot analysis was done to measure the effects of bortezomib on the activations of JNK, ERK and pIRS1 (E). #P<0.05 *vs.* non-treated controls, *P<0.05 *vs.* PA alone, †P<0.05 *vs.* (-) insulin control.

Fig. 5. Effects of AMPK knockdown on the effect of bortezomib on PA-induced ER stress and inflammation. Differentiated C2C12 myotubes were exposed to bortezomib (10 nM) for 1 hr, and then to PA (750 μM) for 24 hr. Western blot analysis was done to measure the effects of bortezomib on the activations of AMPK (A). Interaction between LKB1 and pAMPK was determined by co-immunoprecipitation using rabbit LKB1 antibody (B). AICAR (AC, 1 mM) was used for positive control. AMPK knockdown was carried out by transfection of differentiated C2C12 myotubes with negative control siRNA or AMPK siRNA (20 nM) (C). After transfection, cells were treated with bortezomib (10 nM) for 1 hr and then with PA (750

μM) for 24 hr. The effects of AMPK siRNA on JNK phosphorylation (D) and the protein levels of ER stress markers (E) were determined by western blotting. Levels of TNF-α and IL-6 proteins in culture media were determined by ELISA and the mRNA levels of these proinflammatory cytokines were determined by qPCR (F). Glucose uptakes were measured in the presence of 1 μg/ml insulin to examine the effect of AMPK siRNA on the effects of bortezomib (G). Results are expressed as the means ± SD of three experiments performed in triplicate. #P<0.05 *vs.* non-treated controls, *P<0.05 *vs.* PA alone, †P<0.05 *vs.* control siRNA.

Fig. 6. *In vivo* effects of bortezomib in ob/ob mice. Bortezomib (50 or 200 μg/kg) was orally administrated to ob/ob mice twice a week for 5 weeks, and plasma glucose concentrations were measured weekly (A). At the end of the experiment, oral glucose tolerance and insulin tolerance testing were conducted (A). Tissues and plasma were obtained, and the plasma levels of proinflammatory cytokines (B and C) were measured. The expression levels of ER stress markers in skeletal muscles were measured by western blotting (D), as were the extents of the phosphorylations of AMPK, JNK and Akt (E). *P<0.05 *vs.* vehicle group.

Fig. 7. Proposed model of the mechanism responsible for the protective effects of bortezomib on PA-induced ER stress, inflammation, and insulin resistance in C2C12 myotubes.

Figure 1

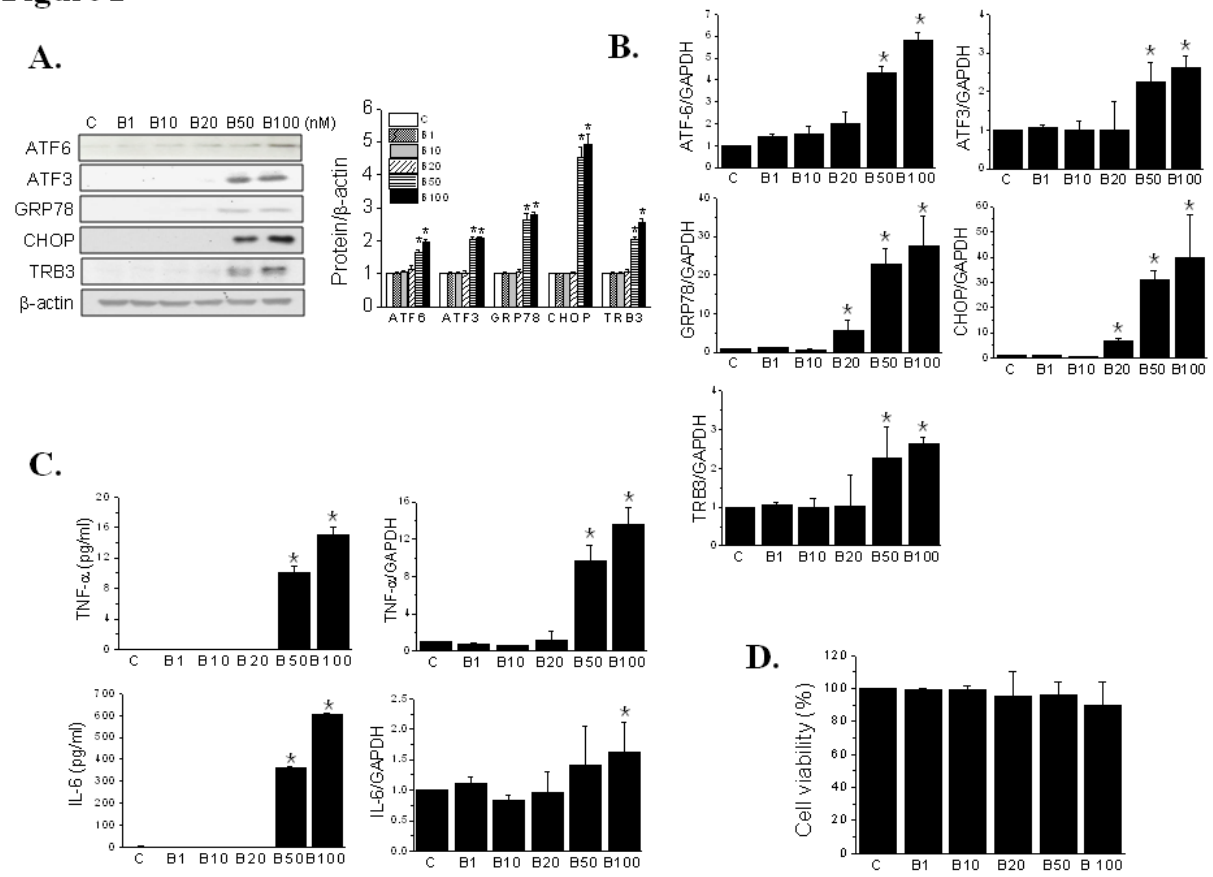

Figure 2

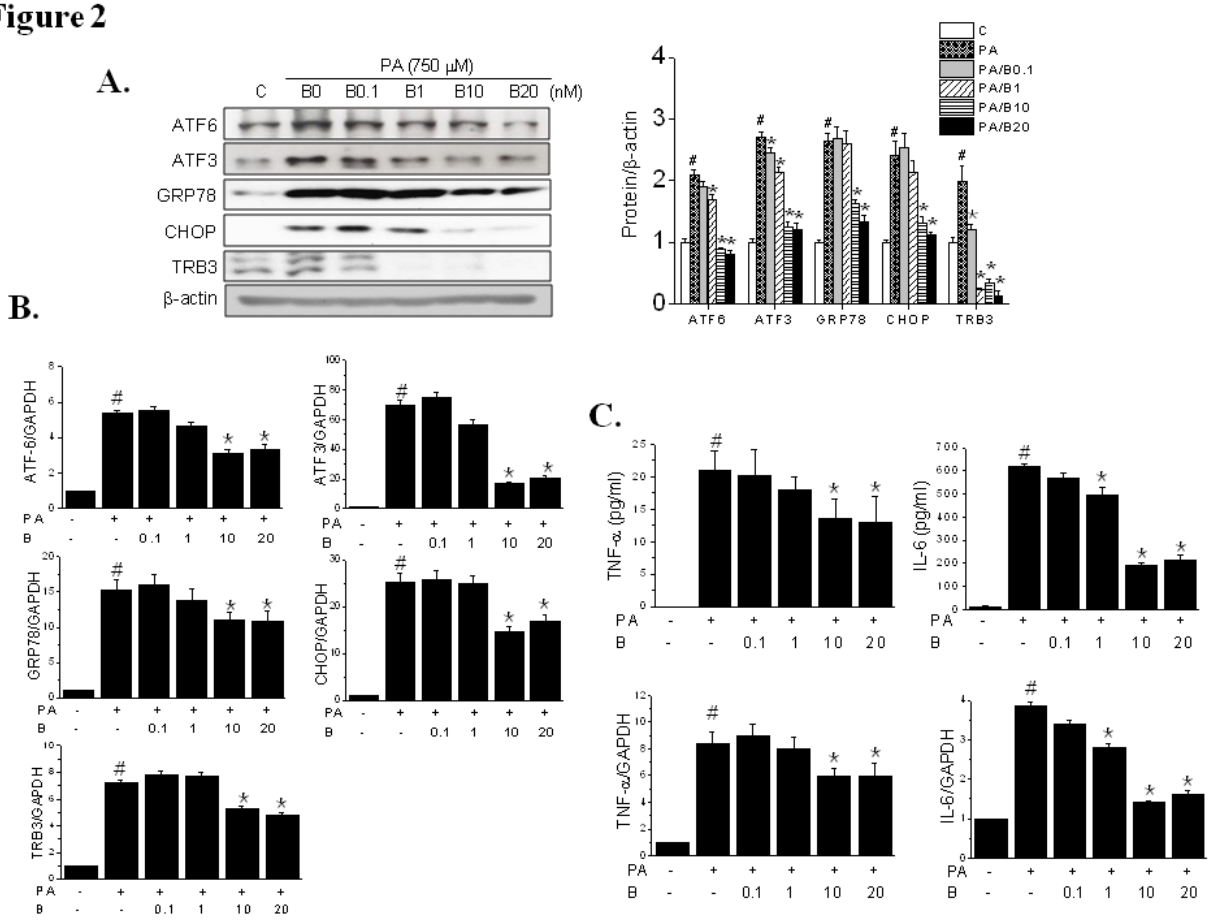

Figure 3

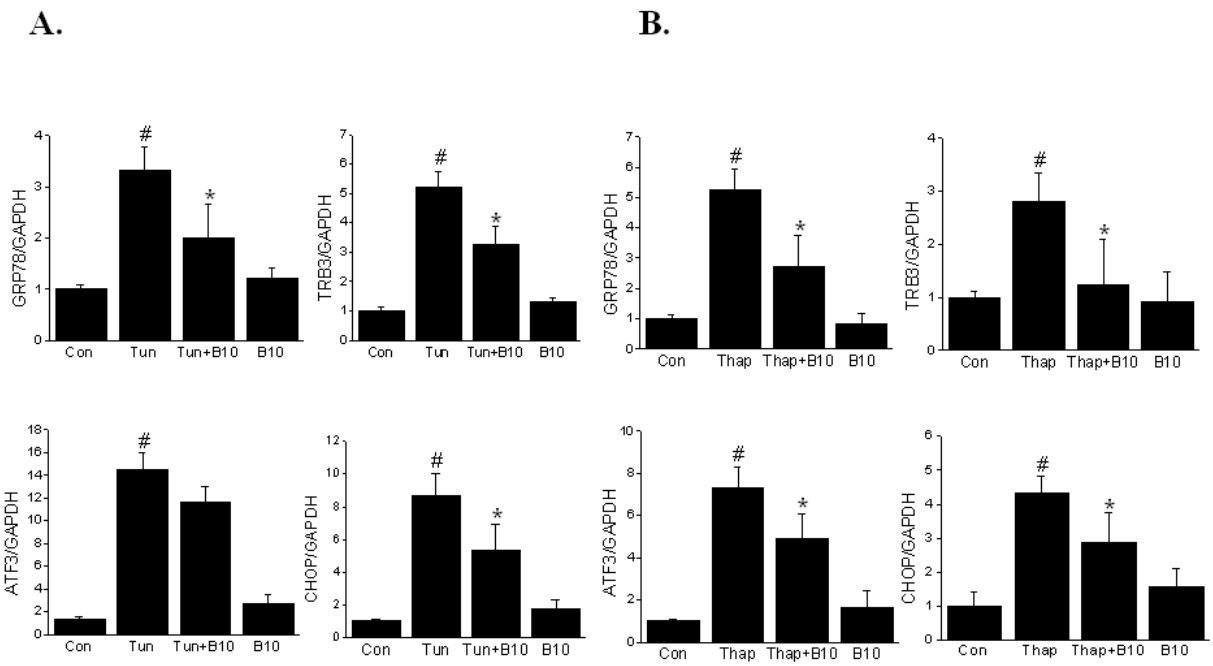

Figure 4

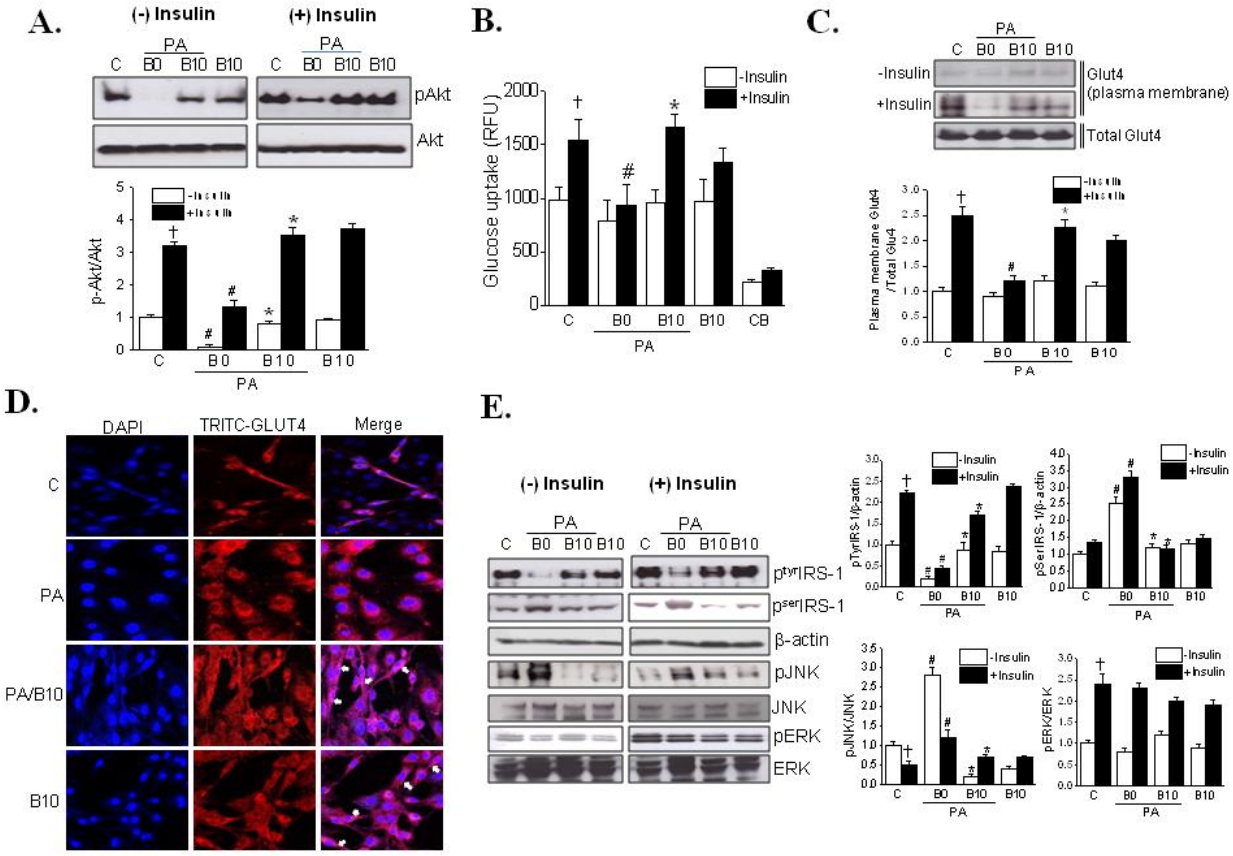

Figure 5

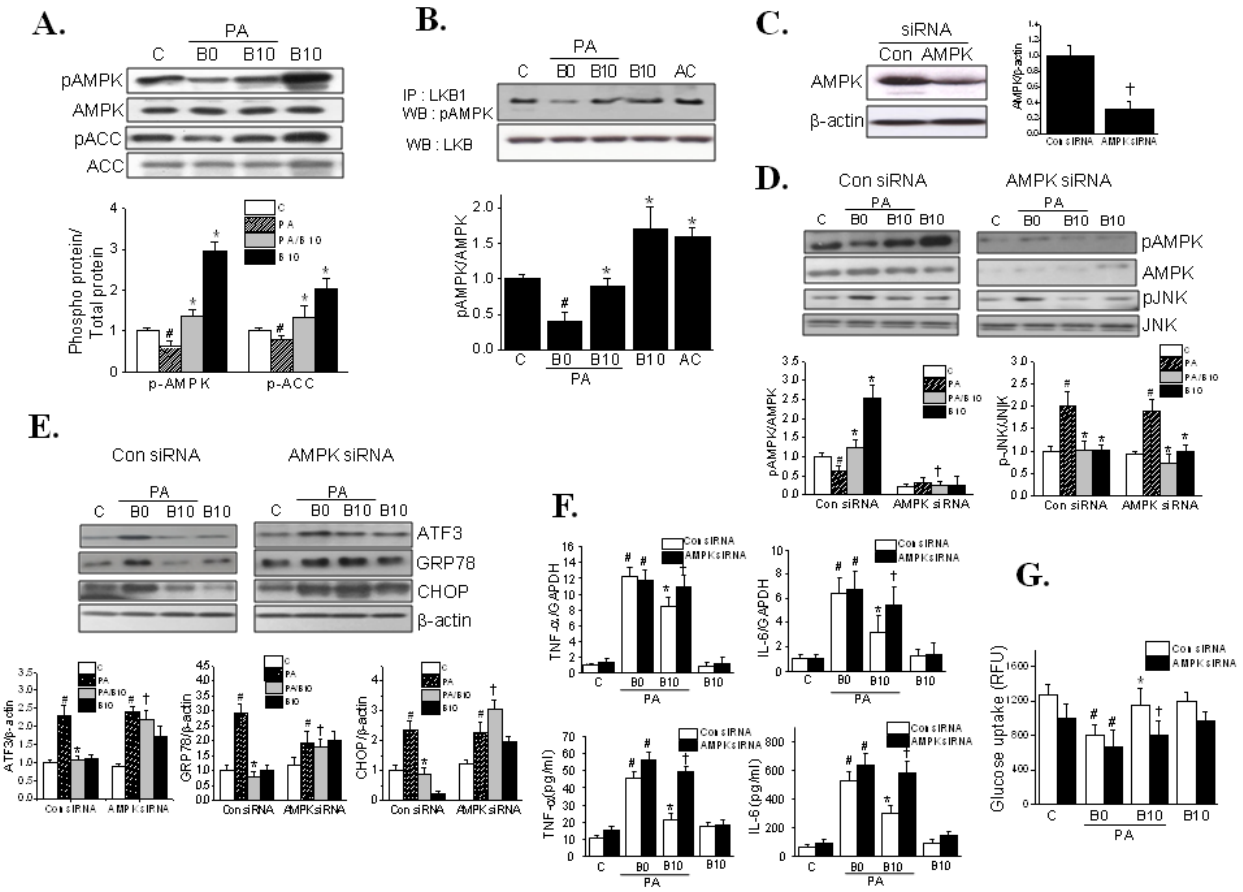

Figure 6

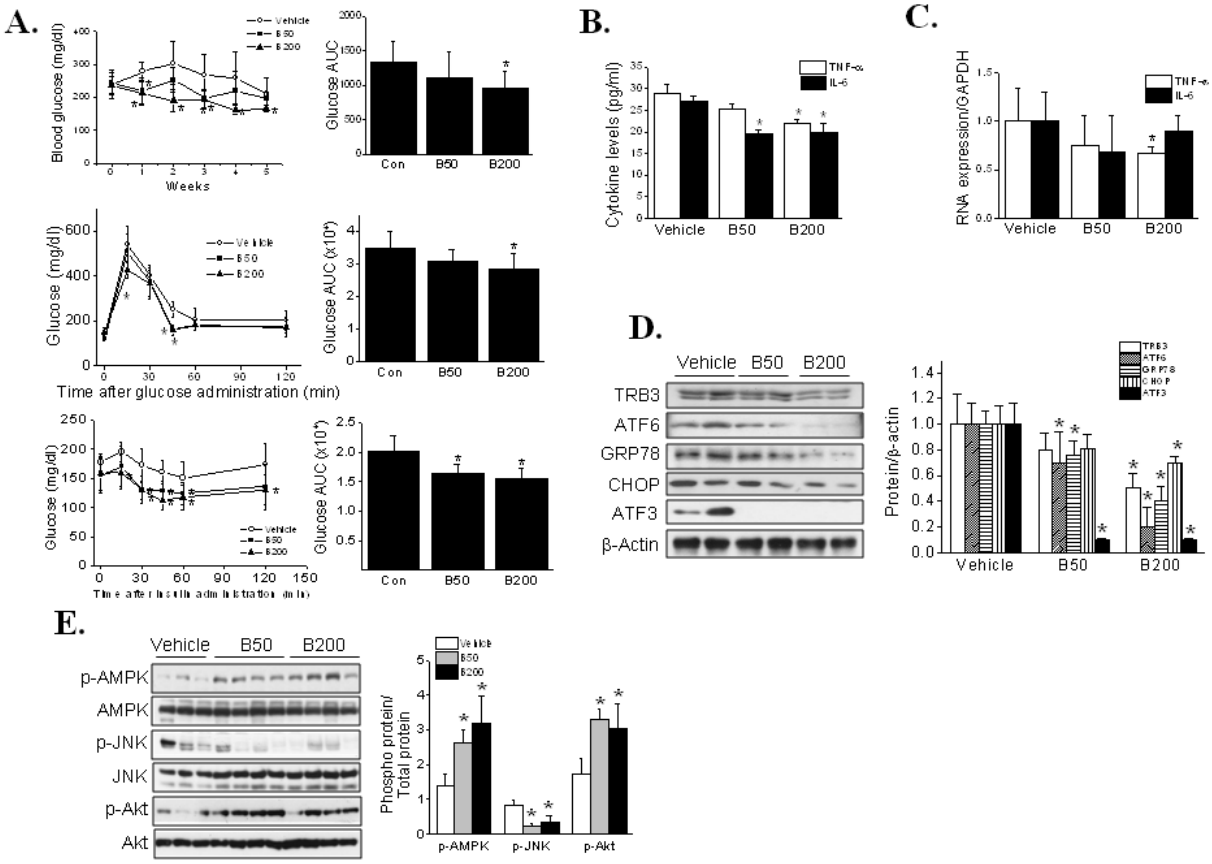

Figure 7

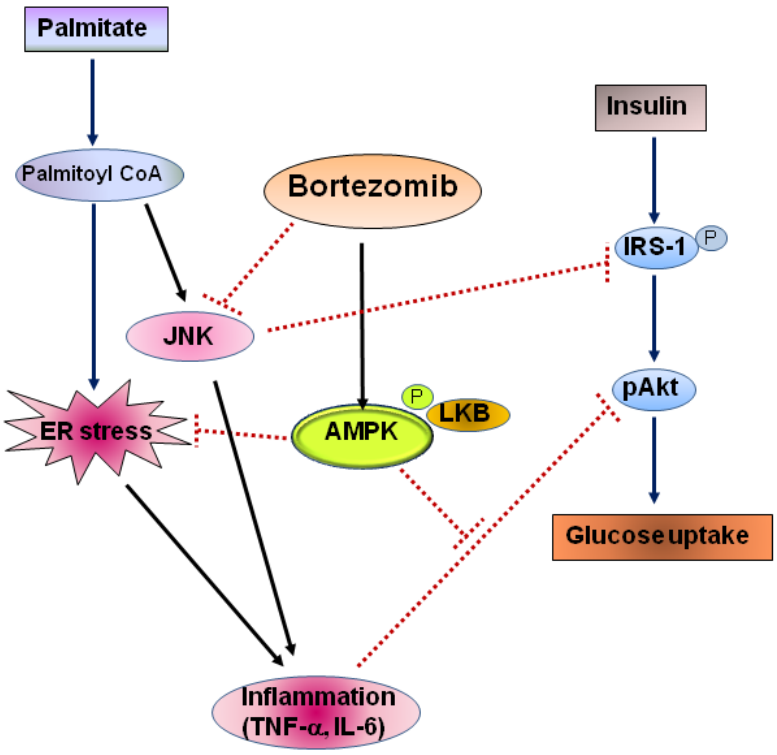

Highlights

- The protective mechanism of bortezomib from palmitic acid-induced damage is proposed.
- Bortezomib reduces palmitic acid-induced ER stress in murine myotubes.
- Bortezomib reduces palmitic acid-induced inflammation in murine myotubes.
- Bortezomib improves palmitic acid-induced insulin resistance in murine myotubes.
- AMPK activation is a key mechanism of the protective action of bortezomib.